

Phase-average analysis of three-dimensional vorticity and temperature dissipation rate in the near field of a heated circular cylinder wake

T. Zhou¹, H. Cao², Y. Zhou^{3,2}, Z. Hao⁴, and L. Cheng¹

¹School of Civil and Resource Engineering, The University of Western Australia,
35 Stirling Highway, Crawley, WA 6009, Australia

²Shen Zhen Postgraduate School, Harbin Institute of Technology, P R China

³Department of Mechanical Engineering, The Hong Kong Polytechnic University,
Hung Hom, Kowloon, Hong Kong

⁴College of Logistics Engineering, Shanghai Maritime University, Shanghai, China 200135

Abstract

In the present study, a probe consisting of four X-type hot wires and two pairs of parallel cold wires was used to measure simultaneously the full energy and temperature dissipation rate as well as the three-dimensional (3D) vorticity components in the near region of a heated circular cylinder wake. The performance of the probe in measuring velocity and temperature fluctuations and vorticity has been checked satisfactorily by comparing the results with those published previously. The vortex structures and the correlation between velocity and temperature fields, the energy and the temperature dissipation rates are analyzed using the phase-average techniques.

Introduction

Turbulence is characterized by high level of fluctuating vorticity, which is usually considered as the least ambiguous quantity for identifying organized structures. However, the measurement of three-dimensional vorticity is not an easy task since multi-hot wires need to be used. The same is true for the energy (ε_f) and temperature dissipation rates (χ_f), which involve multiple hot and cold wires to measure the velocity and temperature gradients in three directions. They are defined as $\varepsilon_f = 2\nu s_{ij}s_{ij}$ and $\chi_f = k\theta_i\theta_i$, respectively, where $s_{ij}(\equiv u_{i,j} + u_{j,i})/2$ is the rate of strain; ν is the kinematic viscosity and $u_{i,j} \equiv \partial u_i / \partial x_j$; k is the thermal diffusivity of the fluid, $\theta_i \equiv \partial \theta / \partial x_i$. The subscript f denote the “full” expressions of the two dissipation rates. In previous studies, significant efforts have been made to measure the 3D vorticity and the energy and temperature dissipation rates in different turbulent flows, albeit not simultaneously (e.g. [1-8]). While it is fraught with difficulties to measure the above two dissipation fields simultaneously, to our best knowledge, there is very little experimental work on the measurement of the above two dissipation rates simultaneously except the ones by Zhou et al. [9] in a decaying grid turbulence and Gulitski et al. [10] in atmospheric surface layer. Direct numerical simulations (DNS) complement experiments in some respects and provide new information on both statistical and structural aspects of the vortical structures since they can resolve complete information on the three-dimensional vorticity and the full energy and temperature dissipation fields. The correlation of the two above dissipation fields can therefore be analyzed using DNS results

[11]. Experimentally, due to the difficulties in managing the multiple hot and cold wires simultaneously, the most common method used to measure the two dissipation rates is employing a single hot wire and a single cold wire by invoking Taylor’s hypothesis i.e.

$$\varepsilon_{iso} = 15\nu u_{1,1}^2 \quad (1)$$

and

$$\chi_{iso} = 3k\theta_{1,1}^2 \quad (2)$$

However, the use of Taylor’s hypothesis has been questioned, especially in high turbulence flows. What is more, significant differences of the above substitutions with their full expression counterparts have been reported previously [12,13].

The first objective of this paper is to measure the full energy and temperature dissipation rates simultaneously in a cylinder wake by using a multiple hot and cold wire probe (Figure 1), which contains eight hot wires and four cold wires. The performance of the probe in measuring velocity, temperature, vorticity, energy and temperature rate is assessed by comparing the present results with those reported previously. On the basis of these measurements, the correlations between the two dissipation fields and the vorticity are further examined (second objective) by using the phase-averaged technique. Differences of the correlations are examined when the full expressions for ε and χ or their isotropic counterparts ε_{iso} and χ_{iso} are used.

Experimental Set-up

The experiments were conducted in a wind tunnel at Nanyang Technological University with a cross-section of 1.2m (width) \times 0.8m (height) and 2 m long. The free stream velocity U_∞ is 3.0 m/s, corresponding to a Reynolds number $Re (\equiv U_\infty d / \nu)$ of 2540, where $d = 12.7$ mm is the diameter of the stainless steel circular cylinder. The measurement locations are at $x/d = 10, 20$ and 40. At these locations, it has been estimated that the Kolmogorov length scales $\eta [\equiv (\nu^3 / \langle \varepsilon \rangle)^{1/4}]$ on the wake centerline are about 0.15~0.3 mm. A heating wire with diameter of about 0.5 mm was wrapped and inserted into a ceramic tube, which was put inside the cylinder as a heating element. The mean temperature increase ΔT on the centerline of the wake at the measurement location, relative to the ambient, is about 1.5°C. This value is small enough to avoid any buoyancy effect and large enough to assure high signal-to-noise ratio.

A probe consisting of four X-probes and two pairs of parallel cold wires (Figure 1) was used to measure the energy and temperature dissipation rates simultaneously. The four X-probes also allow the calculation of all three components of the vorticity vector using the measured velocity signals u_1 , u_2 , and u_3 . With the two pairs of parallel cold wires, the three temperature derivatives $\partial\theta/\partial x_i (i = 1, 2, 3)$ can be measured simultaneously. The included angle of the X-wire is about 100° . The separations Δx_2 and Δx_3 of the two X-probes in the opposite direction are 2mm and 2.7mm, respectively, and the separations Δx_{2c} and Δx_{3c} between the opposite cold wires are about 2.5mm and 2.2 mm. In order to conduct phase-average analysis, another X-probe was used. It was fixed at the outer region of the wake ($y/d = 4\sim 7$) to provide reference velocity signals.

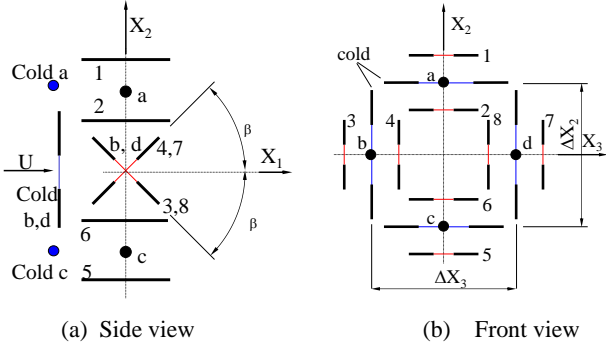


Figure 1: Sketches of the multi-hot and cold wire probe. (a) Side view; (b) Front view.

The hot and cold wires were etched from Wollaston (Pt-10%Rh) wires. The active lengths are about $200d_w$ and $800d_w$ for the hot and cold wires respectively (where d_w is the diameter of the wires and equals to $2.5 \mu\text{m}$ for the hot wires and $1.27 \mu\text{m}$ for the cold wires). The hot wires were operated with in-house constant temperature circuits at an overheat ratio of 1.5. The cold wires were operated with constant current (0.1 mA) circuits. The probe was calibrated at the centerline of the tunnel against a Pitot-static tube connected to a MKS Baratron pressure transducer. The yaw calibration was performed over $\pm 20^\circ\text{C}$. The output signals from the anemometers were passed through buck and gain circuits and low-pass filtered at a frequency f_c of 1600 Hz, which is close to the Kolmogorov frequency $f_K (\equiv U/2\pi\eta)$. The filtered signals were subsequently sampled at a frequency $f_s = 2f_c$ using a 16 bit A/D converter. The record duration was about 60 s.

Results and Discussion

Vorticity and Energy and Temperature Dissipation Rates

The full expression for the full mean energy dissipation rate ε_f , after using the continuity equation, is written as:

$$\begin{aligned} \langle \varepsilon \rangle = & \nu \{ 4\langle u_{1,1}^2 \rangle + \langle u_{1,2}^2 \rangle + \langle u_{2,1}^2 \rangle + \langle u_{1,3}^2 \rangle \\ & + \langle u_{3,1}^2 \rangle + \langle u_{2,3}^2 \rangle + \langle u_{3,2}^2 \rangle + 2\langle u_{1,2}u_{2,1} \rangle \\ & + 2\langle u_{1,3}u_{3,1} \rangle - 2\langle u_{2,3}u_{3,2} \rangle \} \end{aligned} \quad (3)$$

With the four X-wires the three vorticity components were also obtained from the measured u_i signals, viz.

$$\omega_1 = u_{3,2} - u_{2,3} \cong \frac{\Delta u_3}{\Delta x_2} - \frac{\Delta u_2}{\Delta x_3} \quad (4)$$

$$\omega_2 = u_{1,3} - u_{3,1} \cong \frac{\Delta u_1}{\Delta x_3} - \frac{\Delta u_3}{\Delta x_1} \quad (5)$$

$$\omega_3 = u_{2,1} - u_{1,2} \cong \frac{\Delta u_2}{\Delta x_1} - \frac{\Delta u_1}{\Delta x_2} \quad (6)$$

where Δu_3 and Δu_1 in Eqs. (4) and (6) are velocity differences between X-wires a and c, respectively (Fig. 1); Δu_2 and Δu_1 in Eqs. (4) and (5) are velocity differences between X-wires b and d, respectively. Derivatives in the x direction were estimated using Taylor's hypothesis, i.e. $U_1 \partial/\partial x = -\partial/\partial t$. With the two pairs of parallel cold wires (Fig. 1), the three temperature derivatives $\partial\theta/\partial x_i (i = 1, 2, 3)$ can be measured. The full temperature dissipation rate $\langle \chi \rangle$ can be obtained, viz.

$$\langle \chi \rangle = k \{ \langle (\partial\theta/\partial x_1)^2 \rangle + \langle (\partial\theta/\partial x_2)^2 \rangle + \langle (\partial\theta/\partial x_3)^2 \rangle \} \quad (7)$$

As for $\partial u_i/\partial x_1$, $\partial\theta/\partial x_1$ can be determined using Taylor's hypothesis.

Basic Performance Checks of the Probe

The measurements of ε and χ are not straightforward since the velocity and temperature derivatives have to be replaced by using finite differences. It is therefore important to ensure the performance of the probe before any further analysis can be conducted. Figure 2 shows the distribution of the root-mean-square values (indicated by a prime) of u , v and w across the wake normalized by the maximum velocity deficit U_0 and the wake half-width L_0 . It can be seen in Figure 2(a) that the u' values from 4 different X-probes agree reasonably well with each other, especially at the off centerline region. The scatter in the region of $y/L_0 < 1$ is relatively big, though still within the experimental uncertainty. This could be due to the fact that in this region, the turbulence intensity is relatively big, causing more errors in the measurements using X-probes. The agreement of u' from different X-probes at $x/d = 20$ is comparable with that obtained in by Zhou et al. [14] using a probe similar in design to the present one. A similar observation is made for v' and w' , as shown in Figures 2b and 2c, where the values of v' and w' from different cross-wires also exhibit a discrepancy of about 7%. These results indicate that the measurements of u , v , and w from the vorticity probe are quite reasonable. Figure 3 shows the distributions of θ' from the four cold wires normalized by the maximum temperature increase ΔT_0 at the centerline across the wake. The differences of θ' measured by the four cold wires are small and within the experimental uncertainty.

The performance of the probe on the measurement of u , v , w and θ simultaneously can also be checked by examining the joint probability density functions (JPDF) $P_{\alpha,\beta}$ of the signals. The JPDF between two instantaneous signals α and β is defined such that $\iint_{-\infty}^{\infty} P_{\alpha,\beta} d\alpha d\beta = 1$, where α and β represent the fluctuations of the velocity or temperature signals normalized by their rms values. As the separations between the opposite two X-probes (and also the opposite cold wires) are in the order of 2-3mm, it is expected that high correlations exist between the two velocity or temperature signals measured by the opposite wires. This is the case as shown in Figure 3, where the JPDFs of the two velocity or temperature signals measured by the opposite probes are calculated. All the contours show relatively high correlations between the velocity or temperature signals. The correlation

coefficients are all larger than 0.8. The axes of all the JPDF contours are 45°.

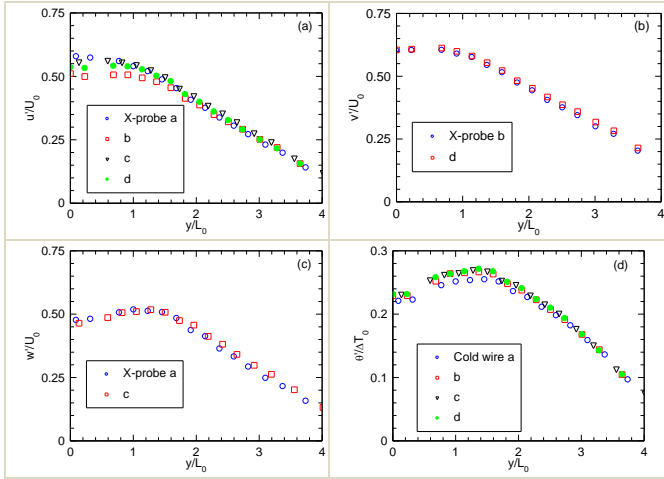


Fig. 2. Rms values of the three velocity fluctuations and temperature fluctuations across the wake measured using the present probe.

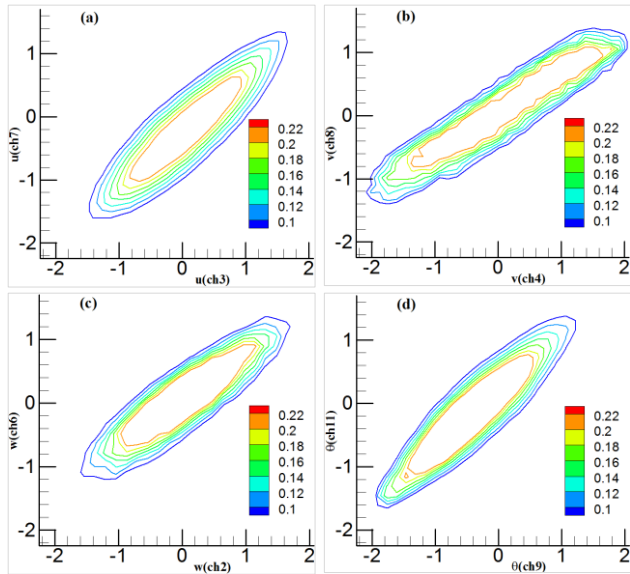


Figure 3. Joint probability density functions $P_{\alpha,\alpha}$ measured at the centerline of the wake. (a) $\alpha = u$; (b) $\alpha = v$; (c) $\alpha = w$; (d) $\alpha = \theta$.

From the measured velocity and temperature signals, the three vorticity components, the energy and temperature dissipation rates can be calculated using Eq (3)-(7). As the finite differences have to be used to approximate the velocity and temperature derivatives, the spectra of the velocity derivatives and the vorticity will be attenuated due to fine wire length and wire separation. This attenuation can be corrected based on the local isotropy assumption. However, in the present study, the measurement locations are at $x/d = 10 - 40$, where local isotropy is not expected due to the existence of the large organized vortical structures. Therefore, the measured velocity and temperature gradients cannot be corrected. To estimate the velocity and temperature gradients more reasonably, care was kept the wire separation in the three directions as close as possible, under the assumption that if there is any spectral attenuation, it will be comparable in all three directions.

The rms values of ω_x , ω_y , and ω_z are shown in Fig. 4. They are normalized by the maximum velocity deficit U_0 and the wake half-width L_0 . To account for the Reynolds number effect, Antonia et al. [15] suggested that $Re_L (\equiv U_0 L / \nu)$ should be included, i.e. $\omega_i^+ = (Re_L^{-1/2}) \omega_i' L / U_0$. The present measurement has been compared with that of Marasli et al.[3] ($x/d = 30$), Mi and Antonia[16] ($x/d = 20$), Zhang et al. [17] ($x/d = 20$) and Zhou et al. [14] ($x/d = 20$). Marasli et al.[3] used a twelve sensor vorticity probe with a spatial resolution of about 2 mm, while Mi and Antonia used two X wires, which were separated by 1.2 mm. The special resolution of Zhang et al. [17] is big, which is about 3.5mm. Zhou et al. [14] used a similar probe with the present with better special resolution than the present one. It can be seen that the agreement between these two studies for $y/L_0 < 1.5$ is satisfactory. In the study by Mi and Antonia [16], the spatial resolution of their probe is good and spectral corrections have been applied. Not surprisingly, their measured values ω_y and ω_z are much higher than those in other studies.

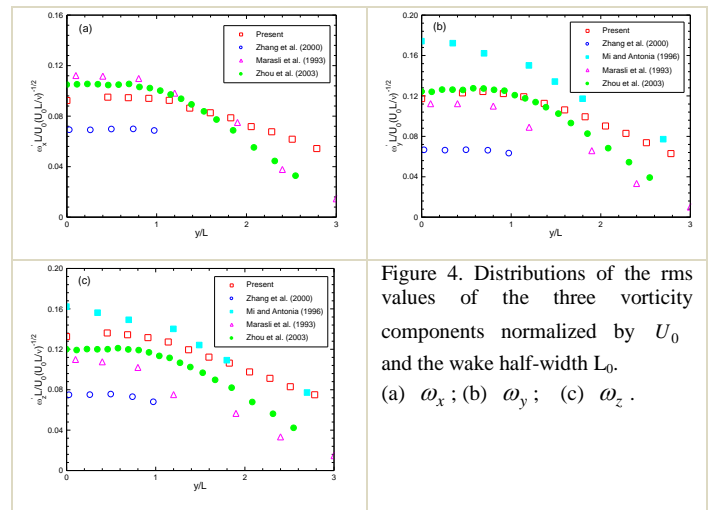


Figure 4. Distributions of the rms values of the three vorticity components normalized by U_0 and the wake half-width L_0 . (a) ω_x ; (b) ω_y ; (c) ω_z .

Phase-average analysis of 3D vorticity and dissipation rates

Using a triple decomposition [17], an instantaneous signal B can be written as the sum of a time-averaged component \bar{B} , a coherent fluctuation $\tilde{\beta}$ and a remainder β_r , viz.

$$B = \bar{B} + \tilde{\beta} + \beta_r, \quad (8)$$

where B stands for instantaneous vorticity and the fluctuation is given by

$$\beta = \tilde{\beta} + \beta_r, \quad (9)$$

The coherent fluctuation $\tilde{\beta}$ reflects the effect from the large-scale coherent structures while the remainder β_r mainly refers to the incoherent structures. The following equation may be derived from Eq.(9):

$$\langle \beta^2 \rangle = \langle \tilde{\beta}^2 \rangle + \langle \beta_r^2 \rangle. \quad (10)$$

The vortical structures in the near and intermediate region of the bluff body wakes are highly periodic. By detecting the vortex shedding frequency and using a reference hot-wire probe to provide reference signals, phase-averaged analysis can be performed. The phase-averaging method is similar to that used by Kiya and Matsumura [18] and Zhang et al. [19].

The phase-averaged iso-contours of the three vorticity components $\tilde{\omega}_x^*$, $\tilde{\omega}_y^*$ and $\tilde{\omega}_z^*$ at $x/d = 10$ are shown in Figure 5, where an asterisk denotes normalization by d and U_∞ . The phase ϕ , ranging from -2π to $+2\pi$, can be interpreted in terms of a longitudinal distance; $\phi = 2\pi$ corresponds to the average vortex wavelength λ . The $\tilde{\omega}_z^*$ contours (Fig. 5c) display the well-known Kármán vortex street (the flow field below the centerline is not shown). The maximum concentration is about 1.15, which is slightly larger than that reported in [14]. The $\tilde{\omega}_x^*$ and $\tilde{\omega}_y^*$ contours (Figures 5a and b) are much weaker than that of $\tilde{\omega}_z^*$ and exhibit little connection to those of $\tilde{\omega}_z^*$. This is probably because phase-averaging is conducted based on the detections of spanwise structures from the v -signal, thus de-emphasizing and even resulting in cancellation between opposite-signed $\tilde{\omega}_x^*$ or $\tilde{\omega}_y^*$ during the phase-averaging process.

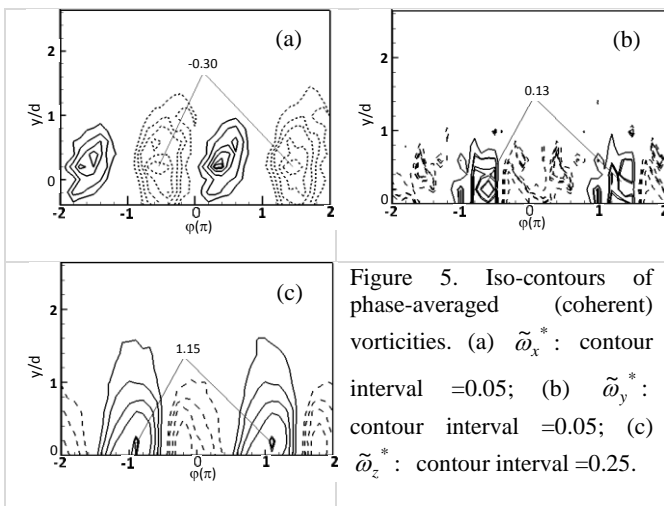


Figure 5. Iso-contours of phase-averaged (coherent) vorticities. (a) $\tilde{\omega}_x^*$: contour interval = 0.05; (b) $\tilde{\omega}_y^*$: contour interval = 0.05; (c) $\tilde{\omega}_z^*$: contour interval = 0.25.

CONCLUSIONS

A twelve-wire probe consisting of eight-hot wires and four-cold wires was used to measure the full energy and temperature dissipation rates simultaneously in the near wake. The performance of the probe in measuring velocity and temperature fluctuations and two dissipation rates and also the three-component vorticity has been verified properly. With the assistance of another X-probe to provide reference signals in the outer region of the wake, phase-average analysis is also conducted. The phase-averaged spanwise vorticity contours show apparent Kármán-type. The vortex structures, the transport of heat and momentum and the correlation between velocity and temperature fields, the energy and the temperature dissipation rates will be analyzed in the future using the phase-average techniques.

References

- [1] Vukoslavčević P., Wallace J.M. & Balint J-L., The velocity and vorticity vector fields of a turbulent boundary layer. Part 1: Simultaneous measurement by hot-wire anemometry. *J Fluid Mech* **228**, 1991, 25-51.
- [2] Tsinober, A., Kit, E. & Dracos, T., Experimental investigation of the field of velocity gradients in turbulent flows. *J. Fluid Mech.* **242**, 1992, 169-92.
- [3] Maralis, B., Nguyen, P. & Wallace, J.M., A calibration technique for multiple-sensor hot-wire

probes and its application to vorticity measurements in the wake of a circular cylinder *Expts. in Fluids* **15**, 209-218.

- [4] Antonia, R.A., Zhou, T. & Zhu, Y., Three-component vorticity measurements in a turbulent grid flow, *J. Fluid Mech.* **374**, 1998, 29-57.
- [5] Zhu, Y. and Antonia, R.A., Performance of a three-component vorticity probe in a turbulent far-wake, *Expts in Fluids* **27**, 1999, 21-30.
- [6] Sreenivasan, K.R., Antonia, R.A. & Danh, H.Q., Temperature dissipation fluctuations in a turbulent boundary layer. *Phys Fluids* **20**, 1977, 1238-1249.
- [7] Anselmet, F., Djeridi, L. & Fulachier, L., Joint statistics of a passive scalar and its dissipation in turbulent flows. *J Fluid Mech* **280**, 1994, 173-179.
- [8] Danaila, L., Zhou, T., Anselmet, F. & Antonia, R.A., Calibration of a temperature dissipation probe in decaying grid turbulence. *Exp in Fluids* **28**, 2000, 45-50.
- [9] Zhou, T., Antonia, R.A. & Chua, L.P., Performance of a probe for measuring turbulent energy and temperature dissipation rates, *Experiments in Fluids* **33**, 2002, 334-34.
- [10] Gulitski, G., Kholmyansky, M., Kinzelbach, W., Lüghi, B., Tsinober, A. & Yorish, S., Velocity and temperature derivatives in high-Reynolds-number turbulent flows in the atmospheric surface layer. Part 1. Facilities, methods and some general results, *J. Fluid Mech.* **589**, 2007, 57-81.
- [11] Wang, L.P., Chen, S. & Brasseur, J.G., Examination of hypotheses in Kolmogorov refined turbulence theory through high-resolution simulations, Part 2. Passive Scalar Field. *J Fluid Mech* **400**, 1999, 163-197.
- [12] Zhou, T. & Antonia, R.A., Approximation for turbulent energy and temperature dissipation rates in grid turbulence. *Phys Fluids* **12**, 2000, 335-344.
- [13] Hao, Z., Zhou, T., Chua, L.P. & Yu, S.C.M., Approximations to energy and temperature dissipation rates in the far field of a cylinder wake, *Experimental Thermal and Fluid Science* **32**, 2008, 791 - 799.
- [14] Zhou, T., Zhou, Y., Yiu, M.W. & Chua, L.P., Three-dimensional vorticity in a turbulent cylinder wake, *Experiments in Fluids* **35**, 2003, 459-471.
- [15] R.A. Antonia, S. Rajagopalan, Y. Zhu, 1996, Scaling of mean square vorticity in turbulent flows. *Exp in Fluids* **20**, 393-394.
- [16] Mi, J. & Antonia, R.A., Vorticity characteristics of the turbulent intermediate wake, *Experiments in Fluids* **20**, 1996, 383-392.
- [17] Hussain A.K.M.F. & Hayakawa M., Eduction of large-scale organized structures in a turbulent plane wake. *J Fluid Mech.* **180**, 1987, 193-229.
- [18] Zhang, H.J., Zhou, Y. & Antonia R.A., Longitudinal and spanwise vortical structures in a turbulent near wake, *Phys. Of Fluids* **12**, 2000, 2954-2964.
- [19] Kiya, M. & Matsumura, M., Incoherent turbulence structure in the near wake of a normal plate. *J Fluid Mech* **190**, 1988, 343-356.

Acknowledgments

Z. Hao acknowledges the financial supported by Science and Technology Commission of Shanghai Municipality (Pujiang Programme, Grant No. 10PJ1404700) and Shanghai Maritime University (Science & Technology Program, Grant No. 20100089).